

Synthesis and brief study of Polyaniline Sn(IV) Phosphate composite material by ion exchange kinetics

Dr. Udai Pratap Singh

Assistant Professor, Department of Chemistry, D. A-V. College, Kanpur

ABSTRACT

For $Mg^{2+}-H^+$, $Ca^{2+}-H^+$, $Sr^{2+}-H^+$, $Ba^{2+}-H^+$, $Ni^{2+}-H^+$, $Cu^{2+}-H^+$, $Mn^{2+}-H^+$, and $Zn^{2+}-H^+$ exchanges at 25, 33, 50, and $65(\pm 0.5)^{\circ}C$ temperatures, ion-exchange kinetics on an electrically conducting organic-inorganic composite cation-exchanger have been studied. Some physical characteristics, including the fractional attainment of equilibrium $U(t)$, self-diffusion coefficients (D_0), activation energy (E_a), and activation entropy (S^*), have been computed as a result. On the surface of this composite cation exchanger at 25, 35, 45 $^{\circ}C$, the thermodynamic adsorption of mancozeb, a fungicide of the class ethylenebisdiethiocarbamate, has also been observed. As a result, it has been possible to evaluate some thermodynamic parameters such as Freundlich constants, thermodynamic equilibrium constants (K_0), standard free energy changes (ΔG^0), standard enthalpy changes (ΔH^0), and standard entropy changes (ΔS^0).

INTRODUCTION

Mercury is a hazardous metal ion with remarkable selectivity. To investigate the cation-exchange model's analytical potential a composite cation exchanger with a mercury selective ion-sensitive membrane known as polyaniline Sn(IV) phosphate has been created and used for analytical experiments. The ion-exchange mechanism of the cation exchange characteristics and electrical conductivity mean-exchanger has yet to be established for the synthesis, physicochemical characterization, and ion exchanger. Kinetic measures are necessary. Studies of the exchange of some divalent alkali and Granth's cation-exchanger, which possessed a better ion-exchange station metal ions, have been conducted to comprehend the mechanism of ion-exchange and its separation location-exchanger Sn(IV) phosphate, which is 1.12 meq dry potential on the surface of the material, with a capacity of 1.96 meq dry g^{-1} as compared to inorganic. Given the preceding-

Given the above facts, it is crucial to investigate some kinetic characteristics, like the diffusion coefficient, energy, entropy, etc. These parameters provide important information about the ion exchange process mechanism, rate-determining step, and rate laws. Furthermore, because of the various effective diffusion coefficients and ion mobilities involved, the earlier approaches to kinetic behaviour are based on the outdated Bt criterion, which could be more beneficial for an accurate ion exchange (non-isotopic exchange) process. The Nernst-Planck equations provide more suitable values for precisely determining the values of the various kinetic parameters with some additional assumptions.

The soil's ability to adsorb substances may be improved by the presence of an ion-exchange material with a high capacity for exchanging ions. An important characteristic has been the adsorption of insecticides on soils. Metal ions impact it, which is crucial in altering the soil's nutritional quality.

Given that inorganic ion exchangers are known to be selective for metal ions, their presence in soil could have various adverse effects. Due to their ion-exchange function, they may significantly impact the retention of metal ions in the soil, restricting their entry into crops and, eventually, the food chain. Pesticides have been discovered to bind to these materials far more strongly than they do to common soils. For instance, antimony(V) silicate made in these labs had ten times greater pesticide carbofuran adsorption potential than soils. This cation exchanger was chosen for the adsorption of pesticides in order to broaden such a study.

Mancozeb, an ethylenebisdiethiocarbamate (EBDC) fungicide, was discovered to bind to the adsorption characteristics of polyaniline Sn(IV) phosphate. Mancozeb guards against various fungal diseases, such as potato blight, leaf spot, scab (on apples and pears), and rust (on roses), in numerous fruit, vegetable, nut, and field crops.

Additionally, cotton, potatoes, corn, sunflower, sorghum, peanuts, tomatoes, flax, and cereal grains' seeds are treated with it. Mancozeb comes in various forms, including dust, liquids, wettable powders, granules that disperse in water, and ready-to-use formulations. It might frequently be discovered with zineb and maneb. It is an insecticide made of organophosphate frequently used in domestic, agricultural, and public health settings to control various insect species.

EXPERIMENTAL

Instruments and Chemicals

The reagents were purchased from Qualigens (India Ltd.), CDH, and Merck. All equilibrium studies were conducted using a water bath incubator shaker with a temperature change of less than $\pm 0.5^{\circ}\text{C}$. Weighing was done using an electronic balance (digital), Sartorius (Japan), model 21 OS.

Creating the Reagents

In demineralized water (DMW), a mancozeb suspension with various molarities ranging from 0.01-0.06M was made.

After making a 0.1N iodine solution in potassium iodide, DMW was used. In MDW and methanol, a 10% lead acetate solution was created using 2N potassium hydroxide.

Polyaniline Sn(IV) Phosphate Preparation

As previously reported, the polyaniline Sn(IV) phosphate composite cation exchanger was created. Equal amounts of a 10% aniline ($\text{C}_6\text{H}_5\text{NH}_2$) solution and 0.1M potassium persulfate ($\text{K}_2\text{S}_2\text{O}_8$) solution produced in 1M HCl were combined to create the organic polymer polyaniline, which was then continuously stirred at 0°C for 30 minutes to produce a green gel. The gel was dissolved into an aqueous solution of 0.1M disodium hydrogen orthophosphate (Na_2HPO_4) and then placed into a white precipitate of Sn(IV) phosphate that had been made at ambient temperature ($25 \pm 2^{\circ}\text{C}$) and $\text{pH}=1$.

The resulting green gel was digested for 24 hours at room temperature ($25 \pm 2^{\circ}\text{C}$). Suction was used to filter the gel after the supernatant liquid had been decanted. Demineralized water (DMW) was used to wash away the excess acid before the material was dried in an air oven at 50°C . To make tiny granules, DMW was used to submerge the dry product. By treating them with 1M HNO_3 for 24 hours while occasionally shaking the mixture and sporadically adding more acid to the supernatant liquid, they were transformed into H^+ forms. After many DMW washes, the extra acid was removed, and it was then dried at 50°C . The material was sieved to a ≈ 25 μm particle size and stored in

desiccators. 1.96 meq dry g^{-1} of the polyaniline Sn(IV) phosphate composite cation-exchanger's

Table 1: Preparation conditions and ion-exchange capabilities of composite polyaniline Sn(IV) phosphate cation-exchange material

Sample	Mixing volume ratio		pH of the inorganic precipitate	0.1M $\text{K}_2\text{S}_2\text{O}_8$ in 1M HCl	10% Aniline in 1M HCl	Appearance of beads after drying	Na^+ ion-exchange Capacity (meq dry g^{-1})
	M $\text{SnCl}_4 \cdot 5\text{H}_2\text{O}$ in 4M HCl	0.1M Na_2HPO_4 In DMW					
S-1	2	3	1.0	1	1	Greenish granular	1.96
S-2	2	3	1.0	-	-	White granular	1.12

In order to guarantee that the composite cation-exchange material was wholly converted to H^+ -form, it was treated with 0.5M HNO_3 for 24 hours at room temperature with intermittent shaking. After numerous DMW washes, the extra acid was eliminated. The dried H^+ -ion exchanger sample was crushed, sieved, and then cut into pieces with specific mesh sizes (25-50, 50-70, 70-100, and 100-125 μm). The particles with mean radii of ≈ 25 μm (50–70 mesh) were selected

from them and utilized to assess various kinetic characteristics. Using a restricted bath approach, the exchange rate was calculated as follows:

In many stoppered conical flasks, 200 mg of the cation-exchanger in H^+ -form was shaken with 20-millilitre fractions of the 0.02M metal ion solutions (Mg, Ca, Sr, Ba, Ni, Cu, Mn and Zn) for various periods (0.5, 1.0, 2.0, 3.0, and 4.0 min.).

When the supernatant liquid was withdrawn, measurements were typically done using EDTA titrations. Each set was performed four times, and calculations were made using the mean values.

Thermodynamics of Adsorption

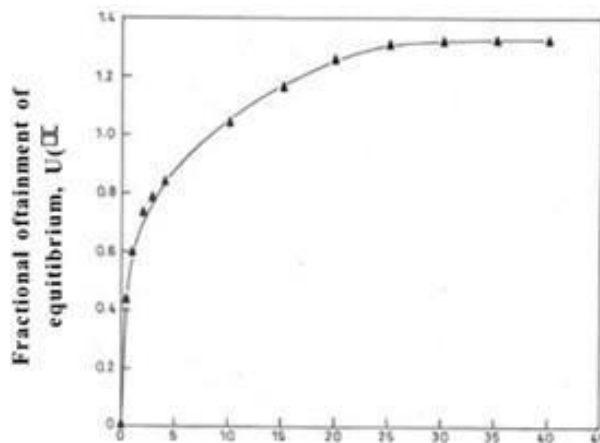
At the desired temperatures (25, 35, and 45°C), 0.5 g portions of the polyaniline Sn(IV) phosphate composite cation-exchanger were added to different stoppered conical flasks. Next, 10 ml mancozeb suspensions at various

concentrations were added, ranging from 0.01-0.06M, and the mixtures were shaken for 70 min each to achieve equilibrium. Iodometric analysis was used to compare the concentrations of mancozeb before and after adsorption, as shown below.

The Cullen system is based on the conventional CS₂ reaction system.

Time/Min

Figure 1 shows a plot of U(t) vs t (time) for M(II)-H(I) exchanges at 33 °C on a composite polyaniline Sn(IV) phosphate cation exchanger to calculate infinite time.



A condenser linked to two traps in sequence by a necked round bottom flask. To help with interference removal, lead acetate [Pb(CH₃COO)₂] solution was added to the first trap after the hydrolysis of the mancozeb was completed. The second trap's methanolic KOH is then used to react with CS₂, and the resulting xanthate is then titrated with an I₂ solution.

CONCLUSIONS AND RESULTS

Metal Ions' Cation-Exchange Kinetics

Kinetic measurements were taken for the exchange of Mg(II)-H(I), Ca(II)-H(I), Sr(II)-H(I), Ba(II)-H(I), Ni(II)-H(I), Cu(II)-H(I), Mn(II)-H(I), and Zn(II)-H(I) under conditions that favoured a particle diffusion-controlled ion-exchange phenomena.

A high metal ion concentration, a relatively large exchanger particle size, and rapid shaking of the exchanging mixture all contributed to the particle diffusion-controlled phenomena.

In an ion exchange process, equilibrium can only be attained with an infinite exchange duration. Over time, the ion exchange rate became independent after Time/min

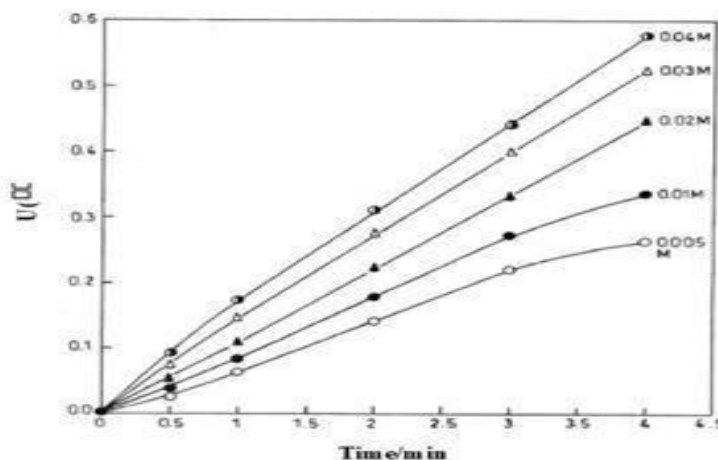


Figure 2 : Plots of U(t) versus t (time) for M(II)-H(I) exchanges using different metal solution concentrations at 33°C on polyaniline Sn(IV) phosphate composite cation exchanger

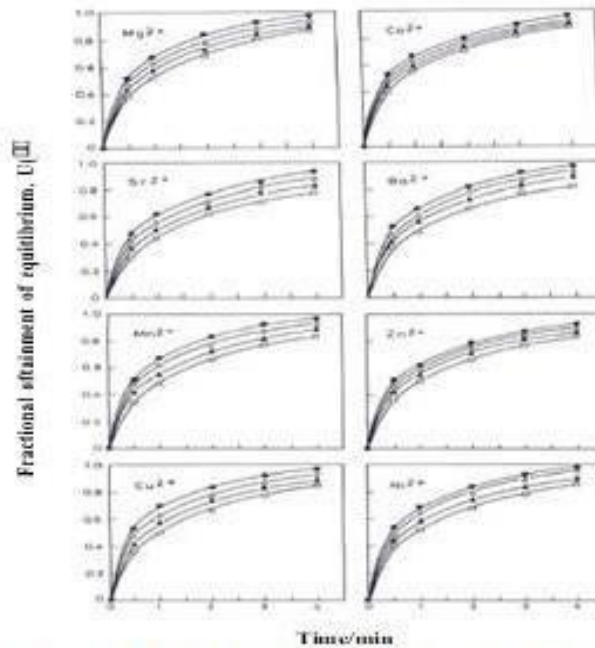


Figure 3 : Plots of $U(t)$ versus t (time) for different $M(II)H(I)$ exchanges at different temperatures on polyaniline Sn(IV) phosphate composite cation-exchanger: (\square) 25°C, (\triangle) 33°C, (\circ) 50°C, (\bullet) 65°C

During this time. Figure 1 depicts the 25 minutes. Were necessary for the $Mg^{2+}-H^+$ exchange to reach equilibrium at 33 C. The same pattern of conduct was seen for Exchanges including $Ca^{2+}-H^+$, $Sr^{2+}-H^+$, $Ba^{2+}-H^+$, $Ni^{2+}-H^+$, $Cu^{2+}-H^+$, $Mn^{2+}-H^+$, and $Zn^{2+}-H^+$. As a result, it was presumed that the system's indefinite exchange time was 25 minutes.

The initial exchange rate was proportional to the metal ion concentration at and above 0.02M, according to a study of the concentration influence on the rate of exchange at 330C (Figure 2). Film diffusion control was more noticeable when the concentration was below 0.02M.

The equation: $U(t)$ = the quantity of trade at time t / The results are represented by the fractional attainment of equilibrium, $U(t)$, with time. (1)

The Volume of Trade Over Infinite Time

For all metal ions, plots of $U(t)$ versus time (t) (t in min.) showed that the fractional attainment of equilibrium occurred more quickly at higher temperatures, indicating that the ions' mobility increased with temperature and their absorption reduced with time. There will be a matching value of a dimensionless time parameter for each U value (t). The numerical findings can be described using an explicit approximation based on the Nernst-Planck equation: $U(t) = \{1 - \exp[\pi^2 (f_1(\alpha) t + f_2(\alpha) t^2 + f_3(\alpha) t^3)]\}^{1/2}$ (2)

Where is the exchange's half-time? $D_{H^+} t/r_0^2$, is the particle radius, D_H and $D_{M^{2+}}$ are the interdiffusion coefficients of the counter ions D_{H^+} and $D_{M^{2+}}$ in the exchanger phase, respectively, and the mobility ratio is defined as $D_{H^+}/D_{M^{2+}}$. The mobility ratio (α) and charge ratio ($Z_{H^+}/Z_{M^{2+}}$) of the exchanging ions affect the three functions, $f_1(\alpha)$, $f_2(\alpha)$, and $f_3(\alpha)$.

As a result, they have various expressions, as seen below. The three functions have the following values when the exchanger is taken in the H^+ -form, and the exchanging ion is M^{2+} , for $1 \leq \alpha \leq 20$, as in this instance.

$$F_1(\alpha) = -1 / 0.64 + 0.36 \alpha^{0.668}$$

$$F_2(\alpha) = -1 / 0.96 - 2.0 \alpha^{0.4635}$$

$$F_3(\alpha) = -1 / 0.27 + 0.09 \alpha^{1.140}$$

Equation (2) is computer-solved to provide the value. The four temperature graphs versus time (t), as shown in Figure 4, are all straight lines that pass through the origin, supporting the particle.

$$S = D_{H^+}/r_0^2 \quad (3)$$

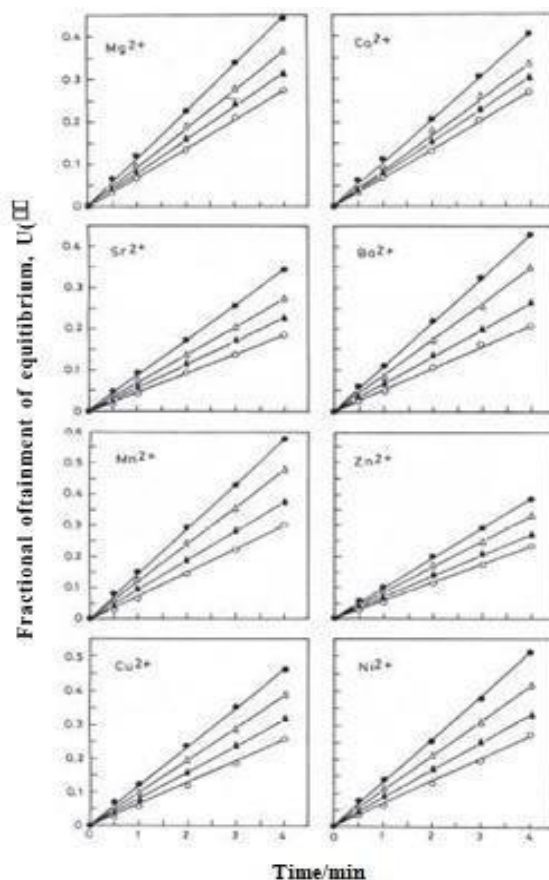


Figure 4 : Plots of $U(II)$ versus t (time) for different M(II)-H(I) exchanges at different temperatures on polyaniline Sn(IV) phosphate composite cation-exchanger: (\square) 25°C, (\blacktriangle) 33 °C, (\circ) 50°C, (\bullet) 65°C

TABLE 2: Slopes of various $U(II)$ versus time (t) plots on polyaniline Sn(IV) phosphate cation-exchanger at different temperatures

Migrating ions	$S (s^{-1}) 10^2$			
	25°C	33°C	50°C	65°C
Mg(II)	6.83	7.83	9.18	11.18
Ca(II)	6.72	7.58	8.51	10.15
Sr(II)	4.56	5.63	6.79	8.58
Ba(II)	5.31	6.65	8.63	10.77
Cu(II)	6.28	7.84	9.59	11.61
Ni(II)	6.60	8.25	10.32	12.70
Zn(II)	5.79	6.76	8.29	9.70
Mn(II)	7.40	9.29	11.87	14.36

$$D_{H^+} = D_0 \exp(-E_a/RT) \quad (4)$$

By extrapolating these lines and utilizing the origin-based intercepts, D_0 is produced. Equation (4) is then used to compute the activation energy (E_a), which results in a value for D_H of 273K. Then, by adding D_0 to equation (5), the entropy of activation (S^*) was computed.

Slopes of different versus time (t) plots on polyaniline Sn(IV) phosphate cation exchanger at various temperatures are shown in TABLE 2.

Ions in motion

TABLE 3: Values of D_0 , E_s , and ΔS^\ddagger for the exchange of H(I) with some metal ions on polyaniline Sn(IV) phosphate composite cation-exchange material

Metal ion exchange with H(I)	10^9 Ionic mobility / $m^2 V^{-1} s^{-1}$	10^2 Ionic radii / nm	$10^7 D_0$ / $m^2 s^{-1}$	$10^2 E_s$ / $kJ mol^{-1}$	ΔS^\ddagger / $JK^{-1} mol^{-1}$
Mg(II)	55	7.8	1.88	68.24	-0.39

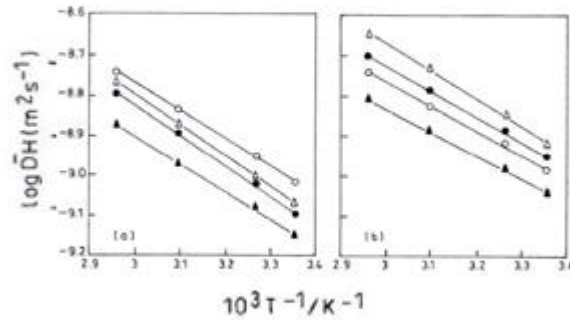


Figure 5 : Plots of $\log D_H$ versus $1000/T$ (K) for (a) Mg (II): \square , Ca(II): \bullet , Ba(II): \square , Sr(II): \blacktriangle , and (b) Mn(II): \square , Ni(II): \bullet , Cu(II): \square , Zn(II): \blacktriangle , on polyaniline Sn(IV) phosphate composite cation-exchanger

$$D_0 = 2.72d^2 (kT/h) \exp(\Delta S^\ddagger/R) \quad (5)$$

Exchanger phase composite for cations

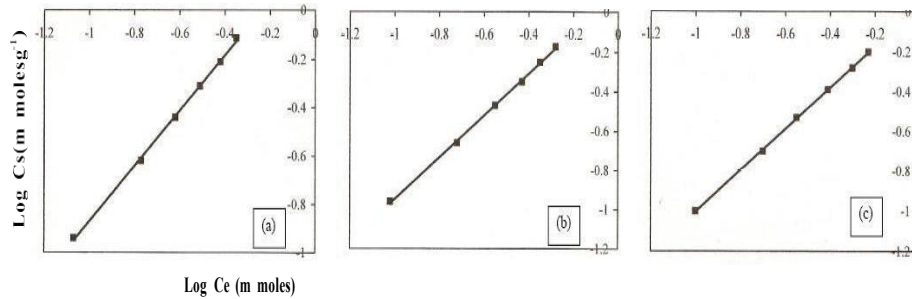


Figure 6 : Freundlich isotherm of mancozeb adsorption on polyaniline Sn(IV) phosphate at 25C (a), 35 C (b) and 45 C (c)

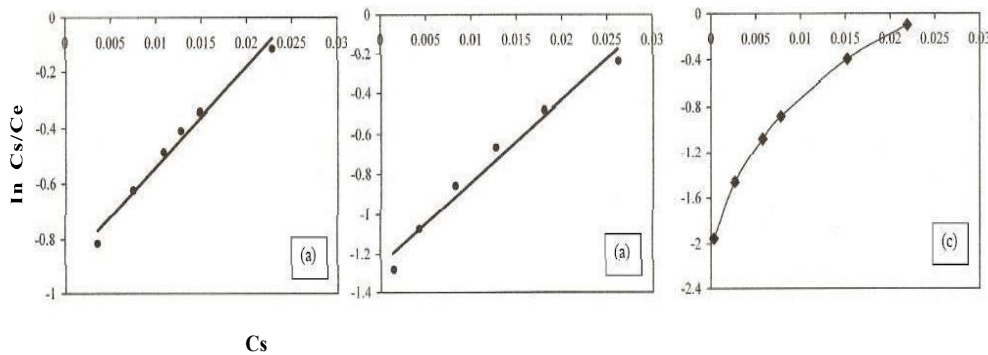


Figure 7 : Plots of $\ln C_s/C_e$ versus C_s on polyaniline Sn(IV) phosphate composite cation exchanger at 25C (a), 35 C (b)

TABLE 4: Freundlich isotherm constants K and 1/n for the adsorption of mancozeb on polyaniline Sn(IV) phosphate composite cation-exchanger

	Temperature (C)		
	25	35	45
K	0.82	0.57	0.85
1/n	1.58	1.51	1.67

TABLE 5: Values of various thermodynamic parameters for the adsorption of mancozeb on polyaniline Sn(IV) phosphate composite cation-exchanger

Thermodynamic constan	Temperature (C)		
	25	35	45
K _o	1.2536	1.2534	1.1963
ΔG (K cal mol ⁻¹)	-0.1336	-0.1380	-0.1131
ΔH (K cal mol ⁻¹)	-0.58	-0.58	-0.58
ΔS (K cal mol ⁻¹ deg ⁻¹)	2.3551 × 10 ⁻³	1.4351 × 10 ⁻³	-1.4682 × 10 ⁻³

Mally expanded the ion-exchange matrix's interstitial locations. Figure 4's plots against time (t) reveal that the straight lines through the origin indicate the particle diffusion phenomena. The entropy of activation values in the negative range indicates that a higher level of order was attained during the forward ion exchange [M(II) - H(I)] process.

Mancozeb's Adsorption Thermodynamics

The equation below is a good representation of the Freundlich adsorption behaviour of the adsorption isotherms at 25, 35, and 450C:

$$x/m = KC^{1/n} \quad (6)$$

Where K and 1/n are constants, C is the equilibrium concentration of mancozeb (m mol ml⁻¹), and x/m is the surface concentration of mancozeb in millimoles per gramme of the exchanger.

This equation predicts that at optimum temperatures, plots of log C_s vs log C_e are straight lines (Figure 6). The constants K and 1/n are obtained from the least squares method fitting the points to the intercepts and slopes of the starting lines, respectively. In TABLE 4, the values obtained are listed.

The variation of the thermodynamic equilibrium constant K_o (known as the thermodynamic coefficient) with temperature change was used to compute the thermodynamic parameters. The adsorption reaction's constant, K_o, can be defined as follows:

$$K_o = a_s / a_e = v_s C_s / v_s C_e \quad (7)$$

A_e is the activity of the solute in solution at equilibrium, whereas it is the activity of the adsorbed solute. Mancozeb's surface concentration (C_s) is measured in m mol per gramme of exchanger; its equilibrium concentration (C_e) is measured in m mol ml⁻¹; its activity coefficients are s for the adsorbed solute and e for the solute in solution.

As the solute concentration in the solution gets closer to zero, the activity coefficient gets closer to unity, which lowers Eq. 7 to the subsequent form:

$$K_o = a_s / a_e = C_s / C_e \quad (8)$$

K_o values are calculated by projecting C_s to zero while charting ln (C_s/C_e) versus C_s (Figure 7). Most minor squares analysis matches the straight line to the points. Its intercept with the vertical axis determines the values for K_o. From the following connection, standard free energy changes (G) for interactions are calculated:

$$\Delta G^0 = -RT \ln K_o \quad (9)$$

T is the temperature in Kelvin, and R is the universal gas constant. The well-known Van t Hoff equation is then used to compute the average standard enthalpy change (H):

Where T₃ and T₁ are two different temperatures, $\ln K_0(T_3) - \ln K_0(T_1) = - \Delta H^0 (T_1 \text{ to } T_3) / R(1/T_3 - 1/T_1)$ (10). Using the equation, standard entropy changes (S) are determined.

$$\Delta G^0 = \Delta H^0 - T\Delta S^0 \text{ (11)}$$

REFERENCES

- [1]. A. A. Khan, Inamuddin; *React. Funct. Polym.*, 66, 1649-1663 (2006).
- [2]. A. A. Khan, Inamuddin; *Sens. Actuat.B: Chem.*, 120, 10-18 (2006).
- [3]. A. Clearfield, A. S. Medina; *J. Inorg. Nucl.Chem.*, 32, 2775-2780 (1970).
- [4]. G. Alberti, R. Bertrami, M. Caseola, U. Costantino J.P. Gupta; *J. Inorg. Nucl. Chem.*, 38, 843-848 (1976).
- [5]. I. P. Saraswat, S.K.Srivastava, A.K.Sharma; *Can. J.Chem.*, 57, 1214-1217 (1979).
- [6]. N. J.Singh, J.Mathew, S.N. Tandon; *J. Phys.Chem.*, 84, 21 (1980).
- [7]. G.E. Boyd, A.W. Adamson, L.S. Myers; *J.Am.Chem. Soc.*, 69, 2836-2848 (1947).
- [8]. D. Reichenberg; *J.Am.Chem.Soc.*, 75, 589-597 (1953).
- [9]. F. Helfferich; *Ion Exchange*, McGraw-Hill, New York, Chapter 6, (1962).
- [10]. W. Nernst; *Z.Physik.Chem.*, 4, 129 (1889).
- [11]. M.Planck; *Ann.Phys.Chem.*, 39, 161 (1890).
- [12]. A. A. Khan, M. M. Alam, F. Mohammad; *Electrochim. Acta*, 48, 2463-2472 (2003).
- [13]. K. G. Varshney, U. Sharma, S.Anwar, A.A.Khan; *Indian J.Chem.*, 23A, 152-154 (1984).
- [14]. K. G. Varshney, A. A. Khan, S.Rani; *Coll. Surf. A: Physicochem. Eng. Asp.*, 25, 131-137 (1987).
- [15]. K. G. Varshney, A. Gupta, K.C.Singhal; *Coll.Surf.A: Physicochem. Eng. Asp.*, 82, 37-48 (1994).
- [16]. P. Gupta, P. K. Varshney; *React.Polym.*, 32, 67 (1997).
- [17]. K. G. Varshney, N. Tayal; *Coll. Surf. A: Physicochem. Eng.Asp.*, 162, 49-53 (2000).
- [18]. A.A.Khan, R. Niwas, M.M.Alam; *Indian J.Chem. Technol.*, 9, 256-260 (2002).
- [19]. A. A. Khan, M.M. Alam, Inamuddin, F. Mohammad; *J.Electroanal. Chem.*, 572, 67-78 (2004).
- [20]. J. W. Biggar, M.W. Cheung; *Soil Sci. Soc. Am.Proc.*, 37, 863-868 (1973).
- [21]. M. Qureshi, K.G. Varshney, (Eds.); *Inorganic Ion Exchangers in Chemical Analysis*, CRC, Boca Raton, Florida, (1991).
- [22]. R. P. Singh, K.G.Varshney, S. Rani; *Ecotoxicol. Environ. Saf.*, 10, 309-313 (1985).